KSCE Journal of Civil Engineering (2023) 27(8):3591-3598
DOI 10.1007/s12205-023-0157-2

pISSN 1226-7988, eISSN 1976-3808
www.springer.com/12205

Tunnel Engineering

Numerical Analysis of Directional Rock Blasting with Continuous-Discontinuous Element Method

Yunpeng Li[a], **Chun Feng**[b], **and Yiming Zhang**[a]

[a]*School of Civil and Transportation Engineering, Hebei University of Technology, Tianjin 300401, China*
[b]*Key Laboratory for Mechanics in Fluid Solid Coupling Systems Institute of Mechanics, Chinese Academy of Sciences, Beijing 100190, China*

ARTICLE HISTORY

Received 14 February 2023
Accepted 9 April 2023
Published Online 17 June 2023

KEYWORDS

Directional rock blasting
Continuous-discontinuous element method (CDEM)
Fracture degree
Damage factor
Numerical simulations

ABSTRACT

When simulating the directional blasting process, many researchers focus on the cutting and splitting effects who might pay more attention on the crushing effects when studying conventional cut blasting. In this case, a numerical tool capable of capturing the strong discontinuity processes of quasi-brittle materials is highly preferable, where many blasting parameters should be calibrated and inputted. In this work, a hybrid finite-discrete elements method with explicit iterative procedure named Continuous-Discontinuous Elements Method (CDEM) is adopted to study the directional rock blasting processes. Landau model is used to capture the detonation effects, where the parameters are calibrated by comparing to the results provided by published literatures. We found that: i) The crack propagation mode of directional rock blasting is similar to those found in Brazilian splitting tests where the crack initiates from the midpoint of the connecting line of blast holes; ii) Compared with traditional cut blasting, the free surface has no significant influence on the blasting effect of directional cut blasting, while the spacing of the hole has great influence on the cutting effect. The index of fracture degree can be used to evaluate the blasting effect quantitatively. This work partly reveals some cracking patterns and rules of directional rock blasting, which may assist the engineers to develop improved precise blasting technologies.

1. Introduction

Directional blasting (Xue et al., 2019; Bhagat et al., 2020) is commonly used in mining engineering, which assures smooth blasting surfaces along the connecting lines of blasting holes at expected positions. Numerical simulations help engineers improve the blasting designs such as explosives and spacing of blasting holes where the numerically-obtained cracking patterns can be used to quantify the blasting effects. Many researchers have also made many achievements with numerical methods. For example: Jiao et al. (2007) studied stress wave propagation in jointed rock using DDA; Hu et al. (2018) developed a 4D-LSM model to study the propagation and attenuation of stress waves in underground chamber explosions; Based on the modified piece-wise Drucker–Prager model, Zhou et al. (2008) studied the dynamic response and damage prediction of concrete slabs.

During blasting, rock fractures are induced by explosive stress wave as well as successive gas pressure. When the former effects create initial cracks around the blasting holes, the latter effects expand the small cracks and split the rocks (Xu et al., 2022). Many sophisticated numerical methods proposed in recent decades can properly capture the initiation, and propagation of cracks in quasi-brittle materials. Some were built in the framework of remeshing (Areias et al., 2013, 2015; Mejia Sanchez et al., 2020), crack/discontinuity embedded (Zhang et al., 2015; Zhang and Zhuang, 2018, 2019; Mu and Zhang, 2020; Zhang and Mang, 2020; Zhang et al., 2021a, 2022), crack/damage degree enriched models (Zheng and Xu, 2014; Miehe et al., 2015; Yang et al., 2016; Wu, 2017; Wu and Nguyen, 2018; Wu et al., 2019). Some others were built in the framework of particle and non-local models (Rabczuk and Belytschko, 2004, 2007; Rabczuk et al., 2010; Fei and Gilles, 2011; Nikolić et al., 2018; Li et al., 2020; Zhao et al., 2020; Zhang et al., 2021b). The mentioned methods have their own advantages and disadvantages in terms of efficiency, stability, complexity, and versa- tility. In our study, we would like to capture the large-scale crack splitting processes during rock

CORRESPONDENCE Chun Feng ✉ fengchun@imech.ac.cn Key Laboratory for Mechanics in Fluid Solid Coupling Systems Institute of Mechanics, Chinese Academy of Sciences, Beijing 100190, China

blasting. The processes last for several microseconds and over hundreds micro cracks can initiate. Large displacement and potential contacts between blasted pieces should also be considered. Considering the efficiency and numerical robustness of explicit iterative procedures when dealing with dynamic fractures, we adopt the Continuous-Discontinuous Element Method (CDEM) (Zhu et al., 2021; Li et al., 2022; Yue et al., 2022) to numerically simulate the directional rock blasting processes. In our case studies, different cut hole spaces are considered. The stress levels, damage and crack degrees are taken to quantify the blasting processes. We found that:

1. Directional fracture blasting will form an obvious compression zone in the direction of the hole connecting line after blast stress wave interference, and induce the crack to extend from the midpoint of the hole connecting line to the adjacent blast hole, which is similar to the law of Brazil splitting.
2. For directional fracture rock blasting, the distance between blast holes is a very important factor. When the hole spacing is too large, the blasting energy can not be effectively concentrated in the direction of the hole connecting line, resulting in poor directional cutting effects.

2. Model

2.1 Basic Principles of CDEM Method

The Continuous-Discontinuous Element Method(CDEM) is a hybrid continuous and discontinuous media calculation method based on explicit integration algorithms. The control equation is:

$$\frac{d}{dt}\left(\frac{\partial L}{\partial \dot{\boldsymbol{u}}}\right)-\frac{\partial L}{\partial \boldsymbol{u}}=\boldsymbol{Q}, \tag{1}$$

where $\boldsymbol{Q}$ is the non-conservative force; $\boldsymbol{u}$ is the displacement; L is the Lagrangian function, which is the sum of kinetic energy, elastic energy and the work done by conservative forces. For a domain Ω, L is

$$L=\frac{1}{2}\int\rho(\dot{\boldsymbol{u}})_i^2 d\Omega+\frac{1}{2}\int\sigma:\varepsilon d\Omega-\int(\int\boldsymbol{f}\cdot\boldsymbol{u}d\boldsymbol{u})d\Omega, \tag{2}$$

where ρ is the density; σ and ε are the stress and stain respectively; $\boldsymbol{f}$ is the physical force.

In the framework of CDEM, the whole domain is discretized by block and interface elements, where each of the latter connecting two of the former. The interface elements are represented by a series of springs, the breakages of which indicate cracking processes, see Fig. 1. If there are joints and other initial cracks in the domain, no springs will be embedded in those positions.

Correspondingly, for these block and interface elements, different material laws are considered. Since rock is considered to be a quasi-brittle material, the block element is described by linear elasticity and the interface element is described by fracture energy model. Both block element model and interface element model are written in incremental form as:

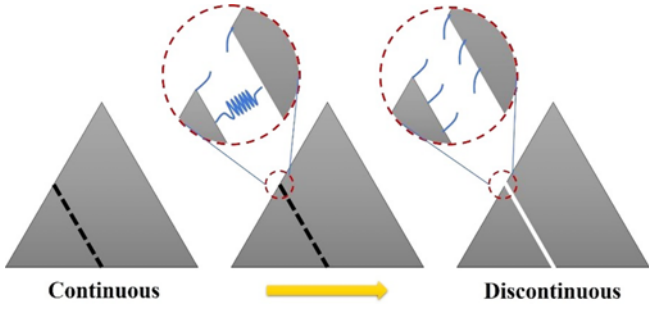

Fig. 1. Elements and Interface Elements Used in the CDEM

2.1.1 For Block Element

$$\begin{cases}\Delta\sigma_{ij}=2G\Delta\varepsilon_{ij}+\left(K-\frac{2}{3}G\right)\Delta\theta\delta_{ij}\\ \sigma_{ij}(t_1)=\Delta\sigma_{ij}+\sigma_{ij}(t_0),\end{cases} \tag{3}$$

where σ_{ij} and $\Delta\sigma_{ij}$ are the total and incremental stress tensors, $\Delta\varepsilon_{ij}$ is the incremental strain tensor; $\Delta\theta$ is the incremental bulk strain; K is the bulk modulus; G is the shear modulus; δ_{ij} is the Kronecker delta; t_1 is the next timestep, t_0 is the current timestep.

2.1.2 For interface element

$$\begin{cases}F_n(t_1)=F_n(t_0)-k_n\cdot A_c\cdot\Delta du_n\\ F_s(t_1)=F_n(t_0)-k_s\cdot A_c\cdot\Delta du_s\end{cases}, \tag{4}$$

where F_n, F_t are the normal and tangential contact forces; k_n, k_s are the normal and tangential contact stiffness; A_c is the area of the interface element; Δdu_n, Δdu_s are normal and tangential relative displacement increments.

The tensile and shear failure states and material rules of the interface element are determined by Eqs. (5) and (6).

$$\begin{cases}if\ -F_n(t_1)\geq\sigma_t(t_0)A_c\\ then\ F_n(t_1)=-\sigma_t(t_0)A_c\\ \qquad\sigma_t(t_1)=-(\sigma_{t_0})^2\cdot\dfrac{\Delta u_n}{2G_{ft}}+\sigma_{t_0},\end{cases} \tag{5}$$

where σ_{t0}, $\sigma_t(t_0)$ and $\sigma_t(t_1)$ are the initial, current, and next time steps tensile strength of the interface element; Δu_n is the normal relative displacement of the interface element at current time step; G_{ft} is the tensile fracture energy.

In addition, three types of damage indicators are defined to describe the types of damage of the interface element as

$$\begin{cases}\alpha=1-\dfrac{\sigma_t(t)}{\sigma_{t0}}\\ \beta=1-\dfrac{c(t)}{c_0}\\ \chi=1-\dfrac{1-\alpha}{1-\beta},\end{cases} \tag{6}$$

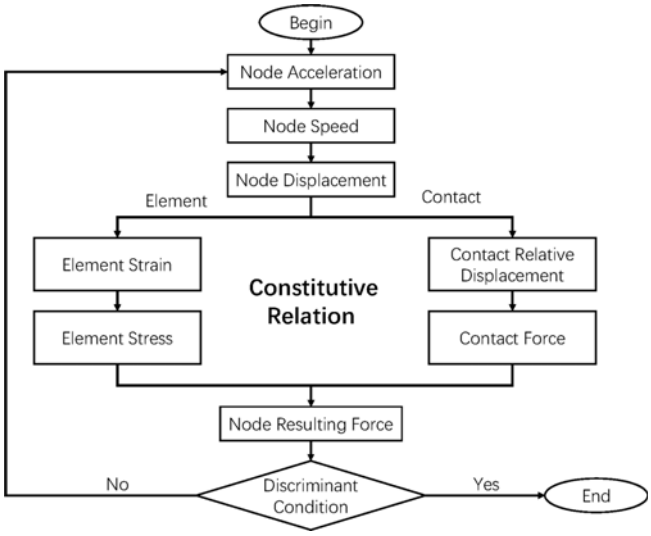

Fig. 2. Flow Chart of CDEM Solution

where α, β and χ are the tensile, shearing, and hybrid damage indicators respectively. When any of these three indicators reaches 1, the interface element will completely break.

The iterative procedure of CDEM is shown in Fig. 2.

2.2 Single Hole Blasting Test

The Landau detonation model is adopted for the blasting loads and the adiabatic expansion model is used for the air adiabatic expansion induced by the blasting. The pressure and volume of the gas are determined by

$$\begin{cases} PV^{\gamma} = P_0 V_0^{\gamma} & P \geq P_k \\ PV^{\gamma_1} = P_k V_k^{\gamma_1} & P < P_k \end{cases}, \tag{8}$$

where P, V are the transient pressure and volume of the high-pressure gas, $(\cdot)_0$ and $(\cdot)_k$ represents the parameters at the initial time step and time step with the boundary pressure P_k. γ and γ_1 are the adiabatic exponents at first and second stages, where $\gamma = 3$ and $\gamma_1 = 1.333$ are taken. The boundary pressure P_k is determined by

$$P_k = P_0 \left\{ \frac{\gamma_1 - 1}{\gamma - \gamma_1} \left[\frac{(\gamma - 1) Q_w \rho_w}{P_0} \right] \right\}^{\frac{\gamma}{\gamma - 1}}, \tag{9}$$

where Q_w is the explosive heat; ρ_w is the charge density.

To test and verify the blasting model, the single hole blasting test studied in (Cho et al., 2008) is simulated. A square PMMA plate (300 mm × 3 00 mm) with a diameter 6.7 mm single blasting hole is considered. Non-reflective boundaries are set on all boundaries. The model is discretized into 5956 triangular block elements and 35736 interface elements, see Fig. 3. The material parameters and blasting parameters are listed in Tables 1 and 2.

We simulate Case C in (Cho et al., 2008). The results are shown in Fig. 4, com-paring to the result provided in (Nakamura, 1999; Cho et al., 2008). Figs. 4(a) – 4(c) show the X-direction

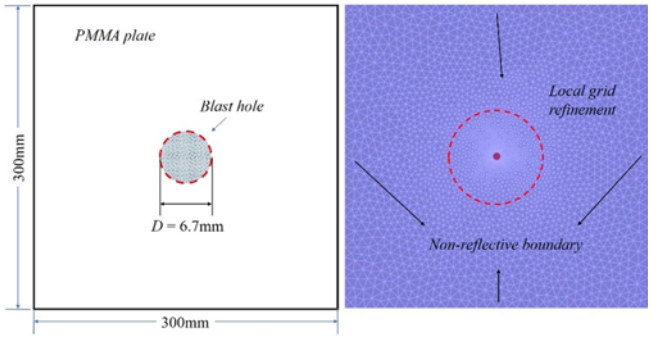

Fig. 3. Numerical Model of PMMA Plate

Table 1. PMMA Plate Main Parameters

Material Properties	Value
Density ρ (kg/m^3)	1,180
Modulus of elasticity E (GPa)	6.1
Poisson's ratio μ (-)	0.31
Cohesive force c_0 (MPa)	30
Tensile strength σ_{t0} (MPa)	30
Tensile fracture energy G_{fi} (Pa·m)	100
Angle of internal friction ϕ (°)	35

Table 2. PETN main parameters

Material Properties	Value
Charge density ρ_w (kg/m^3)	1,770
Explosive heat Q (kJ/kg)	5,895
Boundary pressure P_k (GPa)	3.2

acceleration at different times. It can be found that an instant acceleration of up to $5.0 \cdot 10^5$ m/s^2 was generated around the charge hole after explosion. Then the blasting stress wave propagated when the acceleration decreased. The main crack started to form at around 0.411 μs. There are five main cracks are distributed in a cross shape. In the gaps between these main cracks, there are several shorter radial cracks in the center. The finally obtained cracking pattern shown in Fig. 4(d), whether the number of cracks or the distribution characteristics of cracks, the simulation results in this paper are similar to those which are experimentally and numerically obtained results provided in (Nakamura, 1999; Cho et al., 2008). This test indicates the proposed model can capture the continuous-discontinuous processes of blasting of quasi-brittle materials.

3. Numerical Study of Directional Fracture Rock Blasting

3.1 Model

To study directional fracture rock blasting, a plane with six blasting holes filled with No.2 emulsion explosive is considered, where the diameters of the blast holes are 22.5 mm, see Fig. 5.

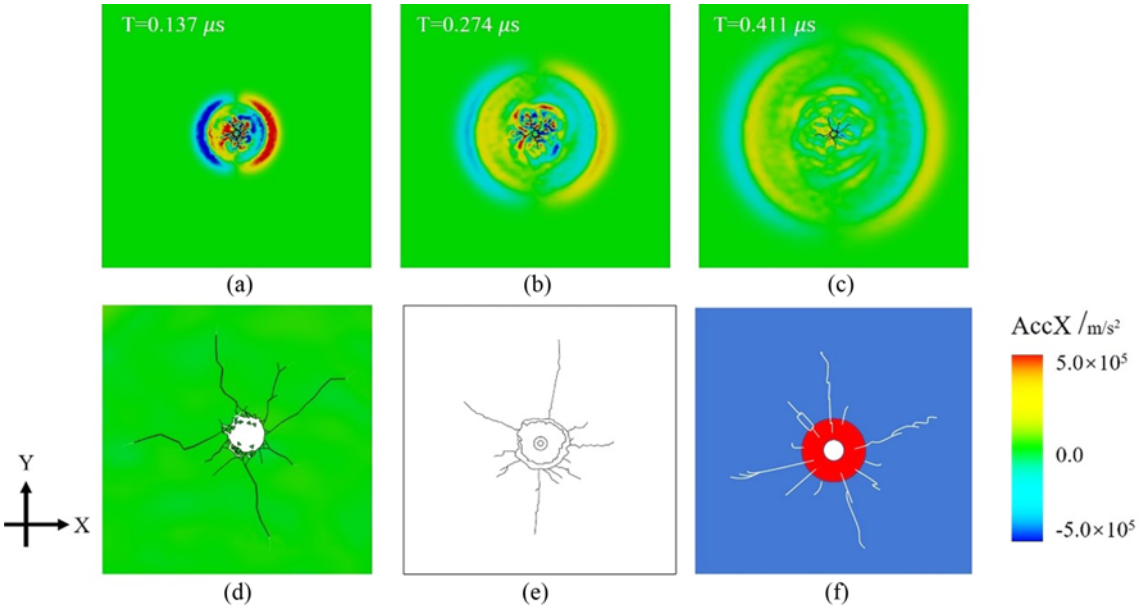

Fig. 4. Single Hole PMMA Plate Blasting Results (Figs. 4(e) and 4(f) are Redrawn Based on the Results from Reference (Nakamura, 1999; Cho et al., 2008), where 4(e) Shows the Experimental Results and 4(f) Shows the Numerical Simulation Results)

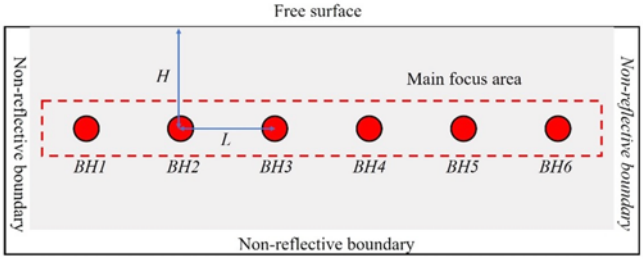

Fig. 5. Directional Fracture Rock Blasting Model

Table 3. Four Cases of Directional Fracture Blasting Design

Scheme number	L/mm	H/mm
Case 1	557	600
Case 2	557	650
Case 3	607	650
Case 4	655	600

Table 4. Rock Main Mechanical Parameters

Material properties	Value
Density ρ (kg/m^3)	2,700
Modulus of elasticity E (GPa)	99.3
Poisson's ratio μ (–)	0.28
Cohesive force C (MPa)	20
Tensile strength T (MPa)	8.11
Angle of internal friction ϕ (°)	56.2
Tensile fracture energy G_{fI} (Pa.m)	500
Shear fracture energy G_{fs} (Pa·m)	1,000

Table 5. No.2 Emulsion Explosive Main Parameters

Material properties	Value
Charge density ρ_w (kg/m^3)	1,150
Explosive heat Q (kJ/kg)	3,100
Boundary pressure P_k (GPa)	70

The three boundaries are non-reflective boundary conditions and the top boundary is free. Considering different H and L, four cases are designed, see Table 3. The mechanical parameters of rock and the main parameters of explosives are shown in Tables 4 and 5.

3.2 Failure Pattern

Case 2 is taken to show the cracking pattern of directional rock blasting. The velocity results are shown in Fig. 6. After explosion, the velocity around the blasting hole reached 50 m/s in a short period. At around 75 μs, the blasting waves of adjacent blasting holes interacted. When the main crack formed along the connecting lines of blasting holes, its width increased very quickly. At around 800 μs, the plane was separated and the upper half block fled at a speed of 30 – 40 m/s.

The minimum principal stress is shown in the Fig. 7. In the beginning of the explosion, high compression stress was formed, leading to radial small cracks around blasting holes. When T = 75 μs, the blast stress wave interfered, and there was no crack in the direction of the hole line at this moment. At T = 100 μs, a compression zone appeared in the direction of the hole line. At this time, the peak pressure in the compression zone was not large, so only small part of the rocks were fractured. Some short transverse cracks first appeared in the center of the hole line. Then, at T = 257 μs, with the interactions of blasting waves from adjacent blasting holes, the peak pressure in the

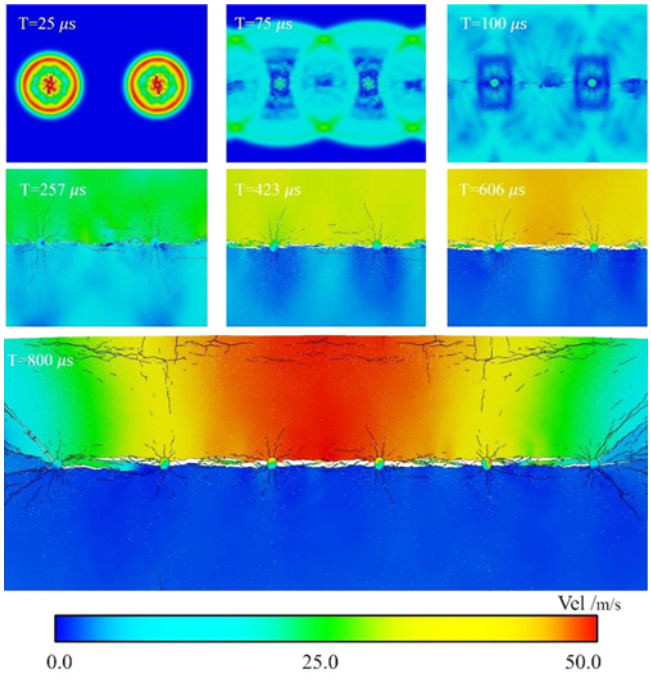

Fig. 6. Velocity at Different Times

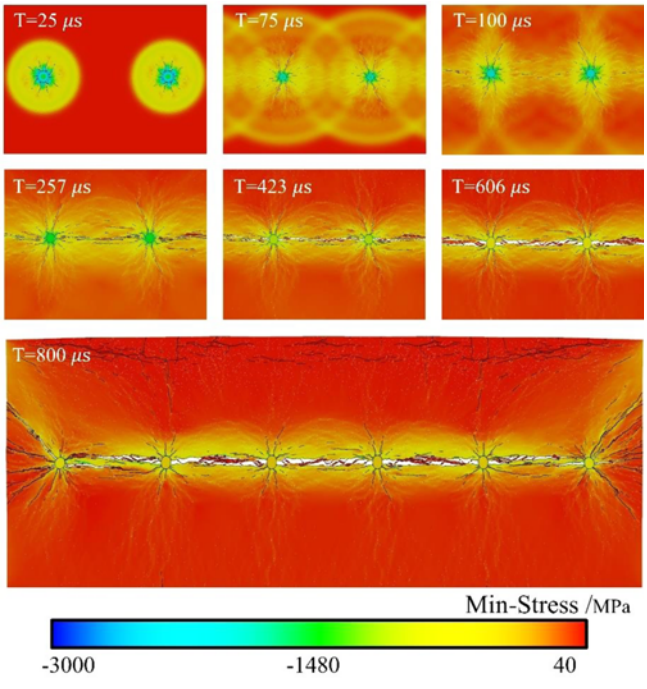

Fig. 7. Minimum Principal Stresses at Different Times

compression zone increases sharply and a large number of rocks were fractured, the main crack formed and stress redistribution occurred.

The damage degrees are shown in Fig. 8. In this figure, 0.0 represents undam- aged and 1.0 represents damaged and cracked. The damage is snowflake shape when the explosive detonated. At around 257 μs, many small cracks appeared before the

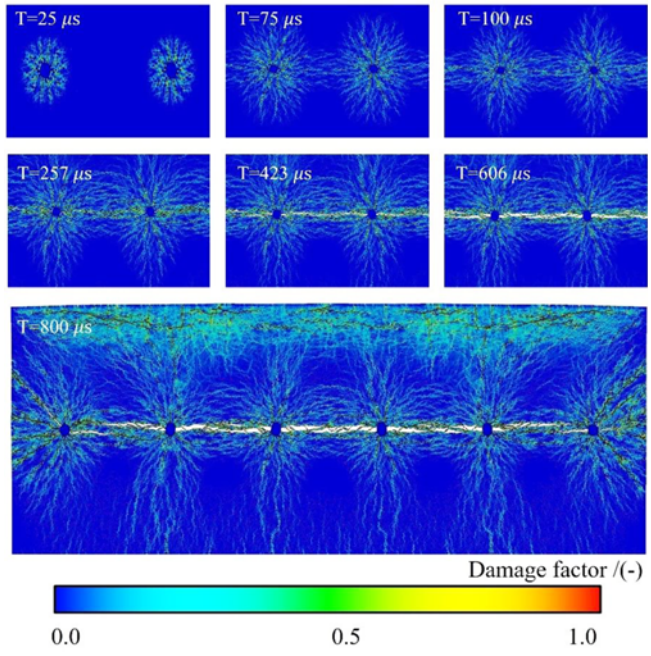

Fig. 8. Damage Degrees at Different Times

formation of main crack.

3.3 Case Studies

Cases 1 to 4 are designed to study the influences of H and L on blasting effects considering the same amount of explosives. The cracking patterns is shown in Fig. 9. In all four cases, there is a crack running through the line of blast hole, and the fracture zone around the hole is small, a relatively complete half-hole shape can still be seen. In general, the results were very similar. The blasting rock fracture shows a splitting crack pattern. Around the blasting holes some radial small tensile cracks appear the length of which is approximately 5 – 10 times the diameter of the blast hole. Because of wave reflection at the free surface, cracks can also be found near the free surface. For same value of H, smaller L (Cases 2 and 3) leads to smooth cracking surface while larger L (Cases 1 and 4) may create zigzag cracking surface and over-break.

The evolution of the fracture degree is shown in Fig. 10, indicating very similar pattern before 280 μs. After 280 μs, Case 4 showed larger damage degrees, mainly induced by the zigzag crack path. Furthermore, to quantitatively evaluate the directional blasting effects, the damage degrees of the rock under the blasting holes are checked and shown in Fig. 11. Within the range of 0.1 m above the blasting holes, damage degree of Case 4 was the highest and that of Case 2 was the lowest. These results indicated that Case 4 may lead to uneconomic overbreak. Cases 2 and 3 were better in which the main crack of Case 3 was longer. Hence, Case 3 gave the best results.

4. Conclusions

In this work, we study the directional rock blasting by a Continuous

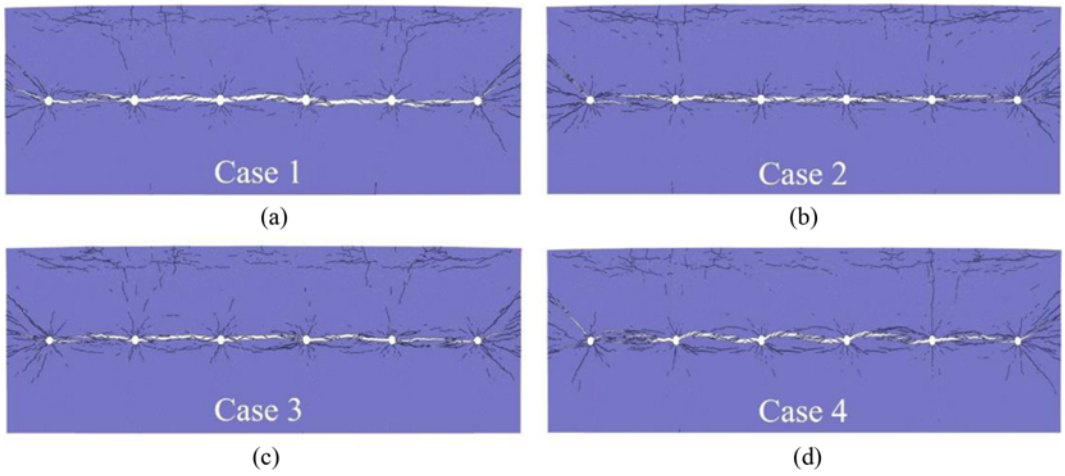

Fig. 9. Four Cases Rock Fracture Diagram

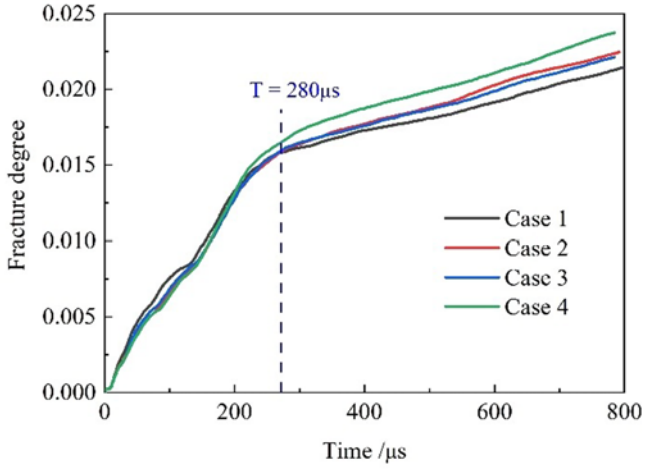

Fig. 10. Four Cases Rock Fracture Diagram

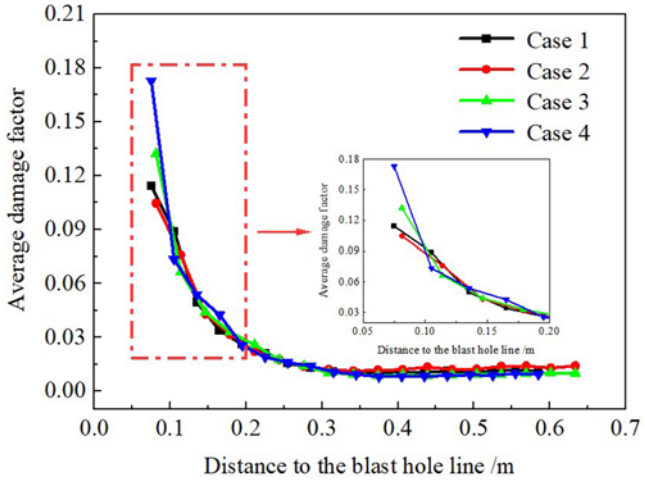

Fig. 11. Average Damage Factor Curve of Four Cases

- Discontinuous Elements Method (CDEM). Considering different blasting designs, some rules are obtained and the best design is determined with qualitative and quantitative studies. The main findings are:

1. Continuous-discontinuous element method can well simulate the continuous-discontinuous process of quasi-brittle material such as rock subjected to blasting loads taking into account large deformations and contact of block elements. The damage of rock can be quantified more intuitively by damage degree.
2. Directional fracture blasting will form a compression zone in the direction of the hole connecting line after blast stress wave interference, and induce the crack to extend from the midpoint of the hole connecting line to the adjacent blast hole. Finally the rock is slit into two blocks.
3. For directional rock blasting, the distance between blast holes is an important fac- tor. When the hole spacing is too large, the directional cutting effect will be poor and zigzag main cracks will appear. Compared with the hole spacing parameter, the distance from the free surface has no significant effect on the blasting effect. By checking the cracking pattern and damage degree, best and most economical design can be obtained.

Acknowledgments

This research was funded by National Natural Science Foundation of China (Grant No.52178324) and National Key Research and Development Project of China, the Ministry of Science and Technology of China (Project No. 2018YFC1505504).

ORCID

Yunpeng Li https://orcid.org/0009-0000-6697-1625
Yiming Zhang https://orcid.org/0000-0002-3693-8039

References

Areias P, Rabczuk T, Dias-da-Costa D (2013) Element-wise fracture algorithm based on rotation of edges. *Engineering Fracture Mechanics*

110:113-137, DOI: 10.1016/j.engfracmech.2013.06.006
Areias P, Reinoso J, Camanho P, Rabczuk T (2015) A constitutive-based element-by-element crack propagation algorithm with local mesh refinement. *Computational Mechanics* 56:291-315, DOI: 10.1007/s00466-015-1172-z
Bhagat NK, Mishra AK, Singh MM, Rana A, Singh PK (2020) Innovative directional controlled blasting technique for excavation of unstable slopes along a busy trans- portation route: A case study of konkan railway in India. *Mining, Metallurgy & Exploration* 37(3):833-850, DOI: 10.1007/s42461-020-00212-x
Cho S, Nakamura Y, Mohanty B, Yang H, Kaneko K (2008) Numerical study of fracture plane control in laboratory-scale blasting. *Engineering Fracture Mechanics* 75(13):3966-3984, DOI: 10.1016/j.engfracmech.2008.02.007
Fei H, Gilles L (2011) Coupling of nonlocal and local continuum models by the arlequin approach. *International Journal for Numerical Methods in Engineering* 89(6):671-685, DOI: 10.1002/nme.3255
Hu XD, Zhao GF, Deng XF, Hao YF, Fan LF, Ma GW, Zhao J (2018) Application of the four-dimensional lattice spring model for blasting wave propagation around the underground rock cavern. *Tunnelling and Underground Space Technology* 82:135-147, DOI: 10.1016/j.tust.2018.08.006
Jiao Y, Zhang X, Zhao J, Liu Q (2007) Viscous boundary of DDA for modeling stress wave propagation in jointed rock. *International Journal of Rock Mechanics and Mining Sciences* 44(7):1070-1076, DOI: 10.1016/ j.ijrmms.2007.03.001
Li Y, Feng C, Ding C, Zhang Y (2022) A novel continuous-discontinuous multi-field numerical model for rock blasting. *Applied Sciences* 12(21), DOI: 10. 3390/app122111123
Li WJ, Zhu QZ, Ni T (2020) A local strain-based implementation strategy for the extended peridynamic model with bond rotation. *Computer Methods in Applied Mechanics and Engineering* 358:112625, DOI: 10.1016/j. cma.2019.112625
Mejia Sanchez EC, Paullo Muñoz LF, Roehl D (2020) Discrete fracture propagation analysis using a robust combined continuation method. *International Journal of Solids and Structures* 193-194:405-417, DOI: 10.1016/j. ijsolstr.2020.02.002
Miehe C, Schänzel LM, Ulmer H (2015) Phase field modeling of fracture in multi- physics problems. Part I. Balance of crack surface and failure criteria for brittle crack propagation in thermo-elastic solids. *Computer Methods in Applied Mechanics and Engineering* 294:449-485, DOI: 10.1016/j.cma.2014.11.016
Mu L, Zhang Y (2020) Cracking elements method with 6-node triangular element. *Finite Elements in Analysis and Design* 177:103421, DOI: 10.1016/j.finel.2020.103421
Nakamura Y (1999) Model experiments on effectiveness of fracture plane control methods in blasting. *Fragblast* 3(1):59-78, DOI: 10.1080/13855149909408034
Nikolić M, Karavelić E, Ibrahimbegovic A, Miščević P (2018) Lattice element models and their peculiarities. *Archives of Computational Methods in Engineering* 25(3):753-784, DOI: 10.1007/s11831-017-9210-y
Rabczuk T, Belytschko T (2004) Cracking particles: A simplified meshfree method for arbitrary evolving cracks. *International Journal for Numerical Methods in Engineering* 61:2316-2343, DOI: 10.1002/nme.1151
Rabczuk T, Belytschko T (2007) A three-dimensional large deformation meshfree method for arbitrary evolving cracks. *Computer Methods in Applied Mechanics and Engineering* 196:2777-2799, DOI: 10.1016/j.cma. 2006.06.020
Rabczuk T, Zi G, Bordas S, Nguyen-Xuan H (2010) A simple and robust three- dimensional cracking-particle method without enrichment. *Computer Methods in Applied Mechanics and Engineering* 199:2437-2455, DOI: 10.1016/j.cma.2010.03.031
Wu JY (2017) A unified phase-field theory for the mechanics of damage and quasi-brittle failure. *Journal of the Mechanics and Physics of Solids* 103:72-99, DOI: 10.1016/j.jmps.2017.03.015
Wu JY, Nguyen VP (2018) A length scale insensitive phase-field damage model for brittle fracture. *Journal of the Mechanics and Physics of Solids* 119:20-42, DOI: 10.1016/j.jmps.2018.06.006
Wu Z, Sun H, Wong LNY (2019) A cohesive element-based numerical manifold method for hydraulic fracturing modelling with voronoi grains. *Rock Mechanics and Rock Engineering* 52:2335-2359, DOI: 10.1007/s00603-018-1717-5
Xu P, Yang R, Zuo J, Ding C, Chen C, Guo Y, Fang S, Zhang Y (2022) Research progress of the fundamental theory and technology of rock blasting. *International Journal of Minerals, Metallurgy and Materials* 29(4):705-716, DOI: 10. 1007/s12613-022-2464-x
Xue H, Gao Y, Zhang X, Tian X, Wang H, Yuan D (2019) Directional blasting fracturing technology for the stability control of key strata in deep thick coal mining. *Energies* 12(24), DOI: 10.3390/en12244665
Yang Y, Sun G, Zheng H, Fu X (2016) A four-node quadrilateral element fitted to numerical manifold method with continuous nodal stress for crack analysis. *Computers and Structures* 177:69-82, DOI: 10.1016/j. compstruc.2016.08.008
Yue Z, Zhou J, Feng C, Wang X, Peng L, Cong J (2022) Coupling of material point and continuum discontinuum element methods for simulating blast-induced fractures in rock. *Computers and Geotechnics* 144:104629, DOI: 10.1016/j.compgeo.2021.104629
Zhang Y, Huang J, Yuan Y, Mang HA (2021a) Cracking elements method with a dissipation-based arc-length approach. *Finite Elements in Analysis and Design* 195:103573, DOI: 10.1016/j.finel.2021.103573
Zhang Y, Lackner R, Zeiml M, Mang H (2015) Strong discontinuity embedded approach with standard SOS formulation: Element formulation, energy-based crack-tracking strategy, and validations. *Computer Methods in Applied Mechanics and Engineering* 287:335-366, DOI: 10.1016/j.cma.2015. 02.001
Zhang Y, Mang HA (2020) Global cracking elements: A novel tool for Galerkin-based approaches simulating quasi-brittle fracture. *International Journal for Numerical Methods in Engineering* 121:2462-2480, DOI: 10.1002/ nme.6315
Zhang Y, Wang X, Wang X, Mang HA (2022) Virtual displacement based discontinuity layout optimization. *International Journal for Numerical Methods in Engineering* 123(22):5682-5694, DOI: 10.1002/nme.7084
Zhang Y, Yang X, Wang X, Zhuang X (2021b) A micropolar peridynamic model with non-uniform horizon for static damage of solids considering different nonlocal enhancements. *Theoretical and Applied Fracture Mechanics* 113:102930, DOI: 10.1016/j.tafmec.2021.102930
Zhang Y, Zhuang X (2018) Cracking elements: A self-propagating strong discontinuumity embedded approach for quasi-brittle fracture. Finite *Elements in Analysis and Design* 144:84-100, DOI: 10.1016/j.finel.2017.10.007
Zhang Y, Zhuang X (2019) Cracking elements method for dynamic brittle fracture. *Theoretical and Applied Fracture Mechanics* 102:1-9, DOI: 10.1016/j.tafmec.2018.09.015
Zhao L, Qiao N, Zhao Z, Zuo S, Wang X (2020) Comparative study of material point method and upper bound limit analysis in slope stability analysis. *Transportation Safety and Environment* 2(1):44-57, DOI: 10.1093/tse/tdaa002
Zheng H, Xu D (2014) New strategies for some issues of numerical

manifold method in simulation of crack propagation. *International Journal for Numerical Methods in Engineering* 97:986-1010, DOI: 10.1002/nme.4620

Zhou X, Kuznetsov V, Hao H, Waschl J (2008) Numerical prediction of concrete slab response to blast loading. *International Journal of Impact Engineering* 35(10):1186-1200, DOI: 10.1016/j.ijimpeng.2008.01.004

Zhu X, Feng C, Cheng P, Wang X, Li S (2021) A novel three-dimensional hydraulic fracturing model based on continuum–discontinuum element method. *Computer Methods in Applied Mechanics and Engineering* 383:113887, DOI: 10.1016/j.cma.2021.113887